Caspian Journal of Environmental Sciences
Online ISSN: 1735-3866
Print ISSN: 1735-3033

# Geostatistical analysis of density indices in traditionally managed oak forests

**Loghman Ghahramany*, Mahtab Pir Bavaghar**

*Department of Forestry, Faculty of Natural Resources, University of Kurdistan; Dr. Hedayat Ghazanfari Center for Research and Development of Northern Zagros Forestry, University of Kurdistan, Sanandaj, Iran*

* *Corresponding author's E-mail: l.ghahramany@uok.ac.ir*

## ABSTRACT

The spatial variation in tree density and basal area provides crucial information for forest health assessment, sustainable forest management, ecosystem monitoring, carbon storage assessment, and climate change mitigation. Literature reviews confirm that geostatistical methods have been effectively applied across various forest management applications. However, their use in traditionally managed oak forests (silvopastoral systems) remains underexplored. The primary challenge in applying these methods lies in the clumped spatial distribution of trees within pollarded oak forests under silvopastoral management.This research applies geostatistical techniques to study the spatial distribution of tree density and basal area in the pollarded oak forests (9,178 ha) of the Northern Zagros region, Northwest Iran, managed under a silvopastoral system. Field measurements were taken in 2019 using a random-systematic sampling design across 117 georeferenced circular plots (0.1 ha each). The mean tree density was 291 stem ha$^{-1}$ (CV = 65.6%), while basal area averaged 14.12 m² ha$^{-1}$ (CV = 49.9%). Variogram analysis showed isotropic behavior and high spatial dependence (SDD = 88% for tree density and 80% for basal area). An exponential model explained 72% and 68% of variability in tree density and basal area, respectively. Small nugget effect values (0.0384 for density, and 0.0476 for basal area) indicated the reliability of the models. Ordinary kriging produced the best predictions, with relative errors of 33.3% (MAEr) and 44.4% (rRMSE) for tree density as well as 30.63% (MAEr) and 41.8% (rRMSE) for basal area. Although higher rRMSE values reflected local deviations, t-test results revealed no significant differences between measured and estimated values. This study underscores the suitability of kriging methods for mapping spatial variations in tree density and basal area, offering valuable approach for forest health assessment and management.

**Keywords:** Density characteristics, Oak forests, Kriging, Spatial structure, Zagros region.
**Article type:** Research Article.

## INTRODUCTION

Effective forest management demands proper assessment of forest structure regarding two key density characteristics: tree density, expressed as the number of trees per unit area, and basal area, defined as the cross-sectional area of tree stems at breast height. These are critical characteristics that are needed for an understanding of forest health, while also informing activities on sustainable management such as wood harvest, thinning, and reforestation; ecosystem monitoring, stress, and decline; the capacity for carbon storage estimates; and the contribution a forest can make in mitigating climate change (Achard *et al.* 2006; Bonan 2008; Buongiorno *et al.* 2012; Newton 2012; Woodall *et al.* 2012; Humagain *et al.* 2017; Hurteau 2021; Ray *et al.* 2023). Traditional methods of ground-based forest inventory, relying on the measurement of reference plots to estimate tree density and basal area, have several limitations. These methods work well in small, easily accessible areas but are time-consuming, expensive, and only provide point estimates. Moreover, they are hard to carry out in remote or inaccessible areas like mountainous regions and are unable to catch the spatial distribution of forest attributes effectively (Scott & Gove 2002; Maselli & Chiesi 2006; SHE *et al.* 2007; Pascual *et al.* 2013; Zhao *et al.* 2022;

Hemingway & Opalach 2024). Given the limitations of traditional inventory methods, there is an increasing demand for more advanced data collection techniques. In this regard, geostatistics—a method of spatial statistics—provides considerable advantages by modeling spatial patterns of forest attributes, such as tree density, basal area, standing stock, tree species composition, biomass, and soil properties. Geostatistics, which uses spatial relationships, can predict values at unsampled locations, significantly enhancing the accuracy of forest maps and parameter estimates. This improved spatial understanding supports more informed and sustainable forest management decisions, including optimizing timber harvesting, planning reforestation efforts, and mitigating climate change impacts (Nanos *et al.* 2004; Tiryana 2005; Freeman & Moisen 2007; Akhavan & Kia-Daliri 2010; Akhavan *et al.* 2014; Raju 2016; Raimundo *et al.* 2017). Geostatistics is an important approach in forest science, being applied in several key areas. It allows detailed mapping of forest inventories, thereby enabling the practice of sustainable forest management even in areas where field data is scanty through robust modeling techniques. This has been shown by Akhavan *et al.* (2010), Yadav & Nandy (2015), Raimundo *et al.* (2017), and Karahan & Erşahin (2017). It is also instrumental in assessing forest health by mapping and monitoring ecosystem diseases, enabling timely decision-making and intervention (Augustin *et al.* 2009; Klobučar & Pernar 2012; Karami *et al.* 2018). Geostatistics is used to project forest growth and yield, considering the existing conditions of the environment (Nanos *et al.* 2004; Raimundo *et al.* 2017; Pelissari *et al.* 2017). It provides an opportunity for soil mapping and characterization, useful for formulating forest management policies, as reflected in Mulder *et al.* (2013), Reza *et al.* (2017), Ahmed *et al.* (2020), John *et al.* (2021), and Selmy *et al.* (2022). Additionally, this helps to assess the effects of climate change on forest ecosystems regarding adapting to changing conditions of weather (Diodato 2005; Meyer *et al.* 2016; Raju 2016; Rehman *et al.* 2022). In recent decades, the application of geostatistics for estimating different forest characteristics has been considered, and we are going to address some of them briefly. Geostatistical methods have largely been applied for mapping different forest attributes and provide essential information for better management and conservation. Among those, these approaches have been previously adopted for the analysis of environmental hazards (Diodato 2005), mapping the site productivity of beech forests (Ahadi *et al.* 2017), and determining stand growth attributes, which includes the volume increment of a stand, the growth increment of diameter, and ingrowth. Additionally, they have been instrumental in mapping the intensity of forest dieback (Karami *et al.* 2018), assessing forest vegetation variability (Olthoff *et al.* 2018), and analyzing soil properties along with their spatial distributions (Ahmed *et al.* 2020; John *et al.* 2021). It has also been applied to mapping forest site indices by Günlü *et al.* (2020), forest canopy metrics by Vafaei *et al.* (2022), and the spatial distribution of aboveground carbon by Izadi & Sohrabi (2022). Other applications include the estimation of aboveground biomass, done by Sales *et al.* (2007), Yadav & Nandy (2015), Babcock *et al.* (2018), and Wu *et al.* (2024); mapping cork productive areas by Montes *et al.* (2005); and basal area, standing forest volumes, tree height, and height-diameter ratios by Nanos *et al.* (2004), Akhavan & Kia-Daliri (2010), and Akhavan *et al.* (2014). These methods have also been applied to site productivity and growth dynamics assessments in a wide range of forest ecosystems. The literature review indicated that geostatistics has been applied to various forest management applications and proved efficient, while in the case of pollarded forests, these methods are less explored. The main challenge to the application of geostatistical methods is the clumped spatial distribution of trees within pollarded oak forests managed under silvopastoral systems. This study explored and evaluated geostatistical methods to model the spatial distribution of stand density and predict stand density at unmeasured locations in a pollarded oak forest in the Northern Zagros region, Northwest Iran. Pollarding is an old, traditional method whereby tree branches and leaves are cut back to produce fodder for livestock and wood for different purposes. Pollarding was developed from ancient times up to the present day. The practice of pollarding is mainly done in Non-Mediterranean Europe, especially in the Pyrenees, Alps, and Basque regions, and is still practiced today in Iran, Greece, Crete, and Sicily. It also widely exists in specific areas of Asia, Africa, South America, and the United States (Burner *et al.* 2005; Rawat & Everson 2013; Alemu *et al*. 2013; Berhe & Tanga 2013; Peri *et al*. 2016). Pollarding is a form of severe pruning that drastically alters the tree's growth, and can stress the plant as a result of disturbing its natural crown structure and growth patterns (Pinkard & Beadle 1998; Ranjbar *et al.* 2011; Khosravi *et al*. 2012; Abbasi *et al*. 2014; Rostami Jalilian *et al*. 2016; Ghahramany *et al*. 2017). Although the pollarding is marginal in some parts of the world, it remains widespread, particularly in arid and semi-arid regions where herbaceous pastures are scarce for much of the year (Alemu *et al*. 2013; Berhe & Tanga 2013; Franzel *et al*. 2014; Geta *et al*. 2014). This study applies geostatistical techniques to estimate the spatial distribution of tree density and basal area in the pollarded oak forests of the Northern Zagros region, Northwest Iran. Key research questions were:

1. How accurate is the estimation of tree density and basal area in pollarded oak forests using geostatistical techniques?
2. Which variogram model best captures the spatial distribution of tree density and basal area in pollarded oak forests?
3. Which kriging interpolation technique provides the best estimates of tree density and basal area in pollarded oak forests?

The findings of this research will, therefore, add to the literature about the spatial distribution of forest density attributes for good and sustainable forest management amidst continuous conservation challenges. The results of this study can be expected to offer useful new information on aspects relating to how spatial modeling may improve the monitoring and management of forests, including in complex systems such as the pollarded oak.

## MATERIALS AND METHODS

### Study area

This study was conducted in a pollarded oak forest located within the Northern Zagros region, Northwest Iran. These forests account for about 449000 hectares of the vast oak forest area measuring about 5,500,000 hectares, which is located on the western parts of Iran. These forests have three main oak species: *Quercus brantii* Lindle, *Quercus libani* Oliv., and *Quercus infectoria* Oliv., and are mixed with coppice and high oak stands (Ghazanfari *et al*. 2004; Marvi Mohajer 2005). These forests are not commercially harvested for their timber, but they play an important role in maintaining ecological balance through erosion control, carbon storage, and regulation of the hydrological cycle. Though such forests protected, local people still harvest these forests for purposes like pollarding, collecting fuelwood, grazing by cattle and harvesting non-timber forest products (NTFPs) such as mature oak acorns, galls of different types and wild pistachio resin. Further, the forested area is also used for agriculture (Jazirehi & Ebrahimi Rastaghi 2003; Ghazanfari *et al.* 2004; Valipour *et al*. 2014; Ghahramany *et al.* 2018). The study area covers an area of 9178 hectares and is bounded by longitudes 45°44'14" to 45°53'22" E and latitudes 35°51'14" to 35°57'45" N. It holds about 7,209 hectares for the forested class while about 1,969 hectares make up the non-forest areas (Fig. 1). The study area consists of low hills with schist, conglomerate, shale, and metamorphosed limestone as parent materials. These soils are representative of the region due to their deep brown color, calcareous in nature. The average annual rainfall in the area is 647 mm, while the average temperature is around 11.4 °C (Shahabedini *et al.* 2018).

### Data acquisition and preparation

#### Field data

This study utilized geostatistical methods to analyze spatial patterns within a network of 117 georeferenced permanent sample plots (each 0.1 ha), established in 2005 and resurveyed in 2019 as part of a multipurpose forest management plan for pollarding in traditionally managed oak forests. The plots were systematically distributed across the study area using a dual-grid sampling design (600×600 m and 670×670 m spacing; Fig. 1) to capture spatial variability in tree density and basal area. All trees with diameter at breast height (DBH) ≥5 cm was measured, allowing for calculation of stand density and basal area parameters. This sampling strategy enabled both evaluation of long-term pollarding effects and comprehensive spatial analysis of forest structure dynamics. The basal area of each tree was determined using the following Equation 1:

$$g_{1.30} = \pi/_{4} \times d_{1.30}^{2} \quad \text{(Equation 1)}$$

where g1.30 is the basal area in cm$^2$ and d1.30 is the DBH in cm.

### Geostatistical Analysis

The fundamental elements of geostatistical analysis are exploratory data analysis, variogram analysis and kriging interpolation method. Exploratory data analysis is an essential step in the geostatistical workflow. It provides valuable insights into spatial distribution, data variability, and outliers (Harris 2017). Geostatistical analysis was performed using data from georeferenced sample plots and their geographic coordinates. The following statistics were calculated to summarize the tree density and basal area distributions: mean, standard deviation, minimum, maximum, coefficient of variation, asymmetry, and kurtosis. Normality tests were carried out to assess suitability for geostatistical analysis using a one-sample Kolmogorov-Smirnov test, quantile-quantile plots, and visual inspections of histograms (Bivand 2010). Because of non-normality, a logarithmic transformation was considered to normalize data on tree density and basal area. To investigate the pattern or trend, the Trend Analysis tool has been executed against density indices data.

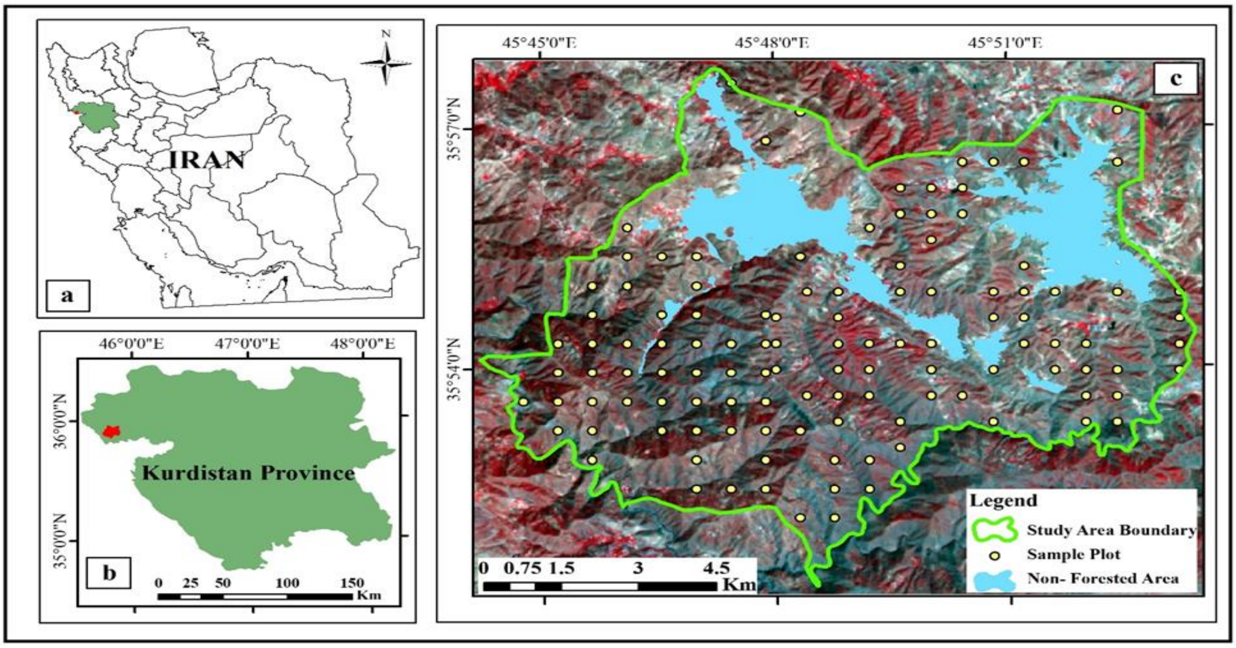


**Fig. 1.** Location of the study area in Iran (a), Kurdistan Province (b), and sample plot's locations within the study area (c) [Image from Landsat 9 (RGB 543)].

Variogram analysis, one of the most important methods in geostatistics, focuses on the spatial autocorrelation of a variable in line with the variation of the observation pairs by a fixed distance between them. This is a statistical procedure used to measure the autocorrelation or dependency between observations concerning their geographical position. Understanding the spatial structure of a variable helps to predict and make better inferences about its behavior at unsampled locations. Fig. 2 explains the estimates of the degree of spatial dependence due to covariance distance between pairs. Semivariance is one of the basic ingredients of variogram analysis. It defines the average squared difference between two observations separated by a specific distance, *h*. (Walter *et al*. 2007; Chiles & Delfiner 2012; Webster & Oliver 2007; Arétouyap *et al*. 2015; Schiappapietra & Douglas 2020). Semivariance is calculated by using Equation 2.

$$\gamma(h) = 1/2 \times \sum_{i=1}^{n(h)} \left[ \left( Z(X_i) - Z(X_i + h) \right)^2 \right] / n(h) \qquad \text{(Equation 2)}$$

where: γ(h): Semivariance at distance h; $Z(x_i)$: Value of the variable at location $x_i$; $Z(x_i+h)$: Value of the variable at location $x_i$ + h (a distance h away); n(h): Number of pairs of points separated by distance h. By fitting a theoretical model to the experimental variogram, we can investigate the spatial structure of the data and make informed decisions about the interpolation and prediction techniques. Spherical, exponential, and Gaussian are common variogram models, each with unique properties (Hengl *et al*. 2007; Chiles & Delfiner 2012). The spatial structure of tree density and basal area was investigated by variogram analysis. Semivariances between pairs of sample plots were computed and plotted against the distance separating them. The best-fitted model was chosen by statistical criteria such as coefficient of determination ($r^2$) and residual sum of squares (RSS). The degree of spatial dependence (DSD) was calculated using equation 3:

$$DSD = \left(\frac{Sill - Nugget\ effect}{Sill}\right) \times 100 \qquad \text{(Equation 3)}$$

Where: Sill represents the total variance of the data and nugget effect is the variance at zero distance.

The spatial dependence degree (SDD) was categorized based on the thresholds proposed by Cambardella *et al.* (1994) and Ganawa *et al.* (2003):

a) Weak structure: SDD < 25%
b) Average structure: 25% ≤ SDD ≤ 75%
c) Strong structure: SDD > 75%

Data isotropy was checked by directional experimental variogram calculation in four directions: 0°, 45°, 90°, and 135°, with a deviation angle of 22°. Anisotropy was checked by superimposing plotted variograms for the mentioned directions and calculating the anisotropy ratio according to Wackernagel (2003), Chiles & Delfiner (2012), Allard *et al.* (2016), Svidzinska (2019), and Verbovšek (2024). The anisotropy ratio was calculated by dividing the maximum range by the minimum range. The anisotropy ratio that indicates isotropy is close to 1. According to Thonon & Cacheiro Pose 2001; Golden Software 2025, the ratio below 2 is considered mild, and a ratio above 4 is rated as severe. Also, the anisotropy in the stand density indices distribution was analyzed using the variogram surface tool in GS+ software (Tiryana 2005). Kriging interpolation method is an interpolation geostatistical method based on data spatial autocorrelation. It is a method of prediction of values to unknown locations as the weighted sum of known observations. In last years, Kriging has been highly used in very different fields as forest sciences. Equation 4 represents the general kriging formula (Webster & Oliver 2000):

$$Z^{*}(\mathrm{X}_0) = \sum_{\mathrm{i}=1}^{\mathrm{n}} \lambda_{\mathrm{i}}\, \mathrm{Z}(\mathrm{X}_{\mathrm{i}}) \quad \text{(Equation 4)}$$

where: $Z^*(x0)$: Predicted value at location $X_0$; $Z(X_i)$: Observed value at location $X_i$; $\lambda_i$: Weights assigned to each observation, determined based on the spatial autocorrelation structure. Different kriging methods are proposed depending on various characteristics of the dataset and assumptions considering the nature of the spatial variability. Every kriging type has particular advantages and will be chosen concerning the specific requirements of the study, nature of data, and application foreseen. The major variants of kriging include, but are not limited to, Ordinary Kriging, Simple Kriging, Global Kriging, and Disjunctive Kriging. Ordinary Kriging (OK) operates under the assumption of an unknown but constant mean, optimizing weights for minimum variance and unbiased predictions (Negreiros *et al.* 2010; Miao & Wang 2024). Simple Kriging (SK) requires prior knowledge of a constant mean, offering computational efficiency when this parameter is known (Siviero *et al.* 2024). For datasets with deterministic trends, Universal Kriging (UK) simultaneously models both spatial structure and trend components (linear/polynomial). Disjunctive Kriging (DK) uniquely handles nonlinear relationships and threshold probabilities by transforming variables while preserving spatial dependence, proving valuable for probabilistic environmental modeling (Oliver *et al.* 1996; Hawchar *et al.* 2018). The validation of interpolation methods ensures the accuracy and dependability of geostatistical models and their predictions. In this research, sample data will be divided into two datasets in order to assess the performance and accuracy of various spatial interpolation models: (i) Training dataset (70% of sample plots, 82 plots): This set was used to model the spatial distribution and develop the interpolation method for estimating density indices; (ii) Validation dataset (30% of the sample plots, 35 plots): This dataset was used to validate and to assess the performance of the interpolation method. The differences between the observed values from georeferenced sample plots and the predicted values in the validation dataset were calculated. Mean error (MAE), relative mean absolute error (rMAE), root mean square error (RMSE), and relative root mean square error (rRMSE) are some of the statistical metrics that have been used to assess the performance of the interpolation method. The equations for MAE, rMAE, RMSE, and rRMSE are given in Equations 5 – 8, respectively. The lower the value of these metrics, the better the accuracy (Oliver & Webster 1990; Heuvelink 1998; Chiles & Delfiner 2012).

$$\mathrm{MAE} = \frac{1}{\mathrm{N}} \sum_{\mathrm{i}=1}^{\mathrm{N}} |\mathrm{z}(\mathrm{X}_{\mathrm{i}}) - \hat{\mathrm{z}}(\mathrm{X}_{\mathrm{i}})| \quad \text{(Equation 5)}$$

$$\mathrm{rMAE} = \frac{\mathrm{MAE}}{\bar{\mathrm{Z}}(\mathrm{X}_{\mathrm{i}})} \times 100 \quad \text{(Equation 6)}$$

$$\mathrm{RMSE} = \sqrt{\frac{1}{\mathrm{N}} \sum_{\mathrm{i}=1}^{\mathrm{N}} [\mathrm{z}(\mathrm{X}_{\mathrm{i}}) - \hat{\mathrm{z}}(\mathrm{X}_{\mathrm{i}})]^2} \quad \text{(Equation 7)}$$

$$\mathrm{rRMSE} = \frac{\mathrm{RMSE}}{\bar{\mathrm{Z}}(\mathrm{X}_{\mathrm{i}})} \times 100 \quad \text{(Equation 8)}$$

Where: N is the number of sample plots, $\hat{z}(X_i)$ is the predicted index value, and $Z(X_i)$ is the measured index value. The actual versus predicted values for tree density and basal area were also compared for the training dataset of 82 sample plots using a paired-sample t-test to further ensure the accuracy of the applied kriging method. The great advantage of the Kriging interpolation method is to give not only the predictions themselves but also the estimate of prediction uncertainty. Based on the variogram model best fitted to the data, prediction maps and standard error maps have been produced accordingly.

**Software Tools**

Descriptive statistics and normality of data were conducted using R-software. Spatial trends analysis in the data on the density indices identified using ArcGIS 10.8. GS+ 5 was utilized to create semivariograms and conduct spatial structure analysis for the stand density. Additionally, geostatistical analysis was performed using ArcGIS 10.8 with the Geostatistical Analyst extension. This included trend analysis, variogram modeling and kriging interpolation conducted through the Geostatistical Wizard. The software was employed to generate prediction maps and associated standard error maps of the studied characteristics.

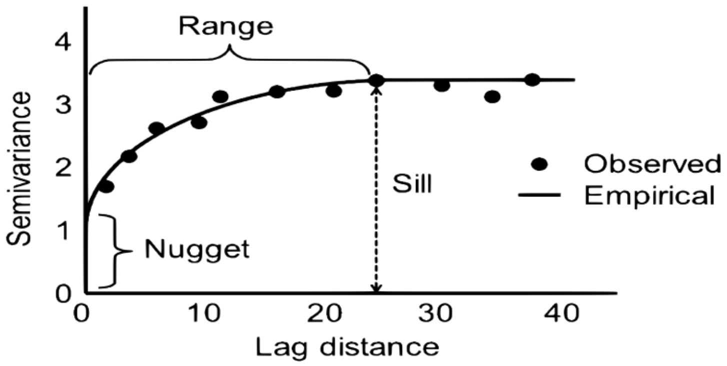


**Fig. 2.** Illustration of a Variogram. The points represent observed data measurements, while the curve depicts the empirical model function. The term "range" refers to the distance at which spatial correlation becomes negligible, "sill" indicates the maximum semivariance value, indicating the overall variability in the data, "nugget" the semivariance value at zero lag distance, representing the inherent variability or measurement error in the data, and the "lag distance" referes to the distance between two data points.

## RESULTS AND DISCUSSION

This study utilized data from permanent sample plots in the study area. The existing dataset met precision requirements for estimating tree density and basal area, with an error margin below 10%. Consequently, no preliminary survey was conducted to determine sample plot quantity or establishment methodology. Fig. 1-c shows the sampling scheme (random-systematic) and the spatial distribution of the georeferenced sample plots in the study area. Summary statistics of density indices from georeferenced sample plots are shown in Table 3. Tree density averaged 291 stem $ha^{-1}$ (with a variation ranging from 100 to 1200 stem $ha^{-1}$) with a coefficient of variation of 65.6%. Basal area averaged 14.12 $m^2\ ha^{-1}$ (ranging from 3.05 to 42.30 $m^2\ ha^{-1}$) with a coefficient of variation of 49.9%. Considering the high density of trees, the low average basal area would then imply a stand dominated by a large number of small-diameter trees. This may be relevant to the coppice structure of the forest and the high density of small-diameter oak sprouts, which are common in this unique ecosystem. Ghazanfari *et al.* (2004) and Ghahramany *et al.* (2018) reported an increase in the abundance and dominance of small-diameter oak sprouts due to traditional management practices that have been going on within the region under study. Tree density and basal area showed high variation and heterogeneity in this oak forest, as described by the coefficient of variation class presented by Dalchiavon *et al.* (2012). Such heterogeneity can be the result of clumped spatial distribution of trees, which has been confirmed in various studies such as Safari *et al.* (2010) and Akhavan *et al.* (2018). Notably, the trees are unevenly distributed within the study area; small-diameter oak sprouts are densely and sparsely distributed in some and other areas, respectively. This distribution is determined by management practices that, in combination with site-specific conditions, affect tree growth and regeneration. Traditional management practices, such as silvopastoral systems, influence forest structure by shaping tree distribution patterns (Villegas *et al.* 2021). Moreover, the widely used practice of pollarding in the studied forest likely influences tree growth and distribution, thus affecting the observed spatial pattern. This has also been asserted by Rostami Jalilian *et al.* (2016) and Ghahramany *et al.* (2017). Such a relationship between forest structure, tree density, growth pattern, and various physiographic features, with shifting soil quality and moisture, was also confirmed by Ghahramany *et al.* (2018). This was also affirmed by the association of environmental variables and species distribution in tropical forests analyzed by Huang *et al.* 2012.

### Trend analysis

Owing to the mountainous nature of the study area, a trend analysis of the density measures was conducted, and the results are presented in Fig. 3. A weak trend in tree density in the north-south and east-west directions and a significant trend in basal area in the west-east direction were identified. However, the inclusion of these trends into the kriging interpolation process did not improve the accuracy of the results. Hence, the trends in the data were excluded to generate the prediction maps and standard error maps for the density indices.

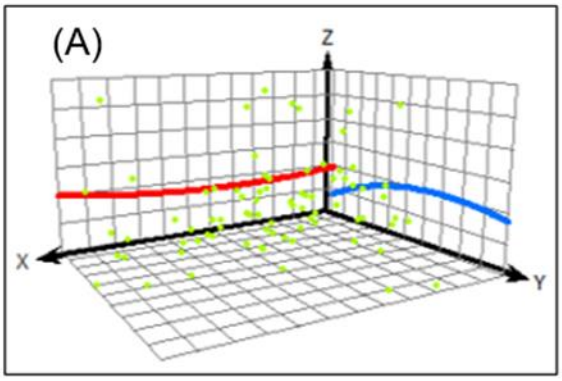


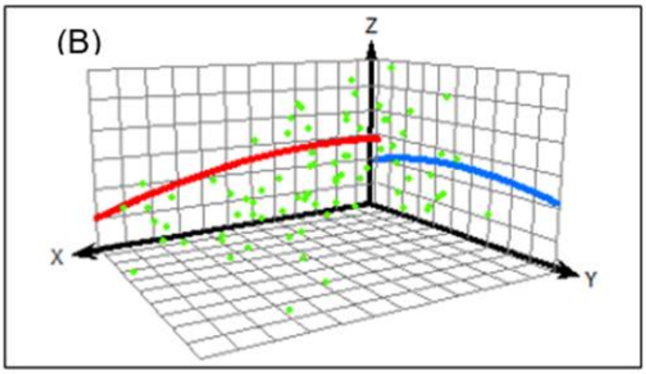


**Fig. 3.** Spatial trends in tree density (A) and basal area (B) field data across the study area in the west-east (X) and the north-south (Y) directions, the Z-axis represents the values of the examined characteristics (tree density or basal area).

**Variogram analysis**

The results of the variogram analysis of tree density and basal area are shown in Table 1. Experimental variograms are reliable in all distance classes with more than 25 data pairs according to the criteria set by Myers (1997). Of the models compared, the exponential model represented in Equation 9 best-described changes in tree density and basal area (Table 1). This is in agreement with a high coefficient of determination and low residual sums of squares that were observed with $r^2 = 0.72$ for tree density and $r^2 = 0.68$ for basal area, RSS = 0.0331 for tree density, and RSS = 0.0126 for basal area. Such results show that the exponential model accounted for 72% of the tree density and 68% of the basal area, while other factors or processes not measured result in the remaining variability (Akhavan & Kiadaliri 2010). Both tree density and basal area showed isotropic behavior, with their anisotropy ratios close to unity, 1.04 and 1.18, respectively (Thonon & Cacheiro Pose 2001; Golden Software 2025). Isotropy was further supported by the symmetric variogram surface shown in Fig. 4; thus, omnidirectional variogram could be used for both examined characteristics during geostatistical modeling (Fig. 5).

$\gamma(h) = C_0 + C\left[1 - \exp(-\frac{h}{R})\right] \Rightarrow h \geq 0$ (Equation 9)

where:

- $\gamma(h)$ is the variogram value at a separation distance h,
- $C_0$+C is the sill (the maximum value that the variogram reaches),
- h is the lag distance (or separation between data points),
- R is the range, which is the distance at which the variogram reaches the sill.

The high values of DSD (88% for tree density and 80% for basal area) indicate that both variables present variability or continuity in space. This characteristic establish them as regionalized variables, fulfilling one of the main prerequisites for applying spatial interpolation methods, confirming that geostatistical methods, such as kriging, are efficient for accurate modeling and prediction according to Ganawa *et al.* (2003) and Appel *et al.* (2018). Despite the strong heterogeneity, strong spatial autocorrelation of tree density and basal area characteristics would thus suggest that this variability is structured rather than random. This structured variability is influenced by environmental factors and traditional management practices (Rozas *et al.* 2009). Understanding these dynamics can support effective management strategies for forests by recognizing the underlying spatial dynamics. The analysis revealed spatial dependence ranges of 1,790 m for tree density and 1,500 m for basal area, representing the maximum distances over which spatial similarity persists (Table 1). Beyond these ranges, the density characteristics become independent. The identified ranges are crucial for determining the dimensions of sampling grids. According to Akhavan & Klein (2009), a distance of two-thirds of the spatial dependence range should be used between sample plots. This information can be used in calculating the dimensions of the sampling grid. For isotropic variograms, a square grid is suitable, while anisotropic variograms necessitate a rectangular grid, optimizing sampling in directions of highest variability. There were nugget effect values of 0.0384 and 0.0476 for the tree density and basal area, respectively. These values were low, which meant that very little variance could not be accounted for by the models, usually because of measurement errors or small-scale spatial variation that increases the reliability of the models (Webster & Oliver 2007). The differences in sill values show greater spatial variability for tree density compared to basal area at 0.3198 for tree density and 0.2392 for basal area. This variability is probably due to such factors as soil fertility, topography, and disturbances by fire or management practices. In contrast, basal area variability is seen to be less in the sense of the homogeneous age structure of the forest (Ghahramany *et al*. 2018).

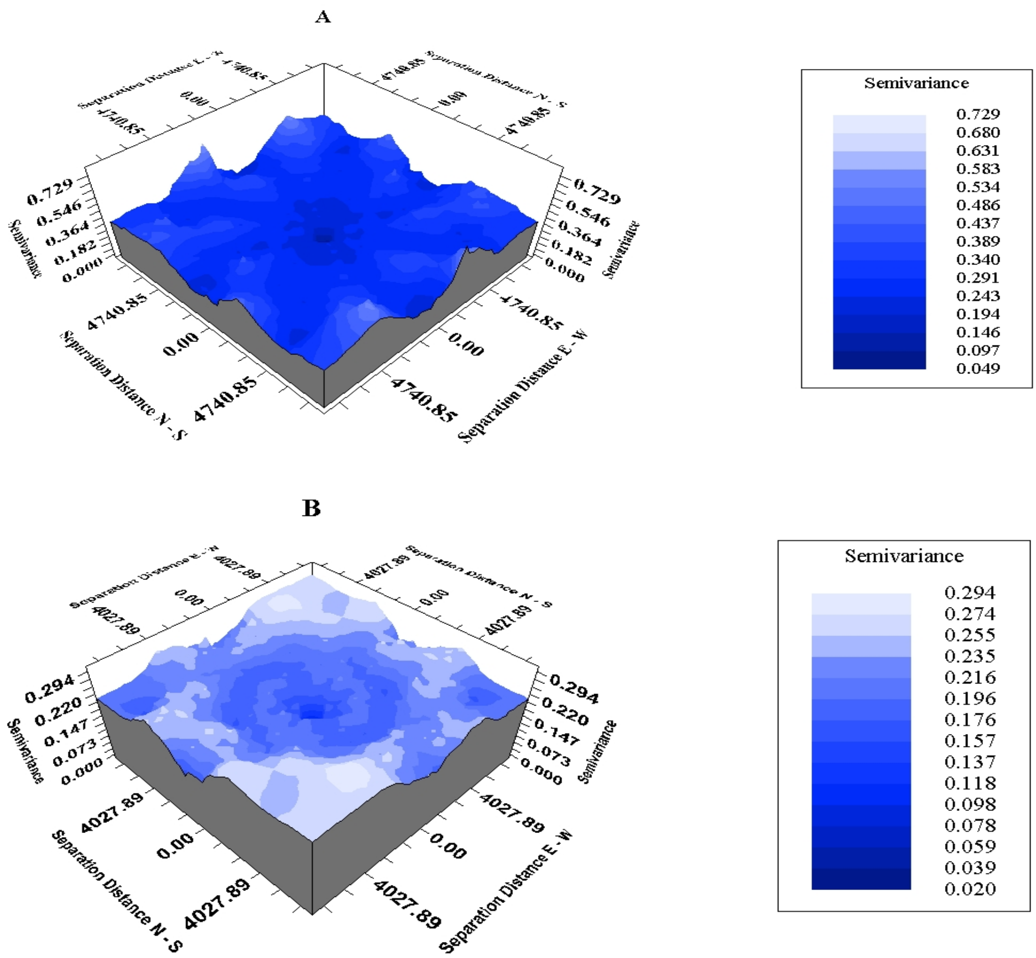


**Fig. 4.** Surface variogram maps in the west-east (W-E) and north-south (N-S) directions, calculated for tree density (A) and basal area (B).

**Table 1.** Result of variogram analysis for tree density and basal area.

| Index | Fitted model | (Co) | (C) | Co + C | A0 (m) | SDD (%) | Ar | $r^2$ | RSS |
|---|---|---|---|---|---|---|---|---|---|
| Tree density (stem $ha^{-1}$) | Exponential | 0.0384 | 0.2814 | 0.3198 | 1790 | 88 | 1.04 | 0.72 | 0.0331 |
| | Spherical | 0.1490 | 0.3300 | 0.4790 | 19590 | 68.9 | - | 0.641 | 0.0422 |
| | Gaussian | 0.1970 | 0.9210 | 1.1180 | 19730 | 82.4 | - | 0.538 | 0.0543 |
| Basal area ($m^2$ $ha^{-1}$) | Exponential | 0.0476 | 0.1916 | 0.2392 | 1500 | 80 | 1.18 | 0.68 | 0.0126 |
| | Spherical | 0.1109 | 0.1369 | 0.2478 | 6950 | 55.2 | - | 0.62 | 0.0149 |
| | Gaussian | 0.1217 | 0.1227 | 0.2444 | 3000 | 50.2 | - | 0.58 | 0.0169 |

Note: Co: nugget effect; C: Structural variance; Co + C: sill; A0: range of spatial dependence; SDD: Spatial dependence degree according to Ganawa *et al.* (2003); Ar: Anisotropy ratio; $r^2$: coefficient of determination; RSS: residual sum of squares.

### Comparison of kriging interpolation techniques

Table 2, illustrates the validation results of some kriging interpolation techniques, including ordinary kriging, simple kriging, global kriging, and disjunctive kriging for predicting tree density and basal area. Among them, ordinary kriging has the best performance in terms of lowest relative errors, rMAE = 33.3% and rRMSE = 44.4% for tree density, and rMAE = 30.63% and rRMSE = 41.4% for basal area. As a result, ordinary kriging was used to produce prediction maps and the corresponding prediction standard error maps for both tree density and basal area, as shown in Figs. 6 and 7. The estimated tree density and basal area derived using ordinary kriging are summarized in Table 3. Although ordinary kriging demonstrated moderate rMAE for tree density and basal area, the high rRMSE values clearly indicate significant variability and heterogeneity in the data. These might be improved by increasing sample size and using stratified ground sampling methods and may improve the accuracy of the estimated density index; hence, these are worthy of further studies in subsequent research works.

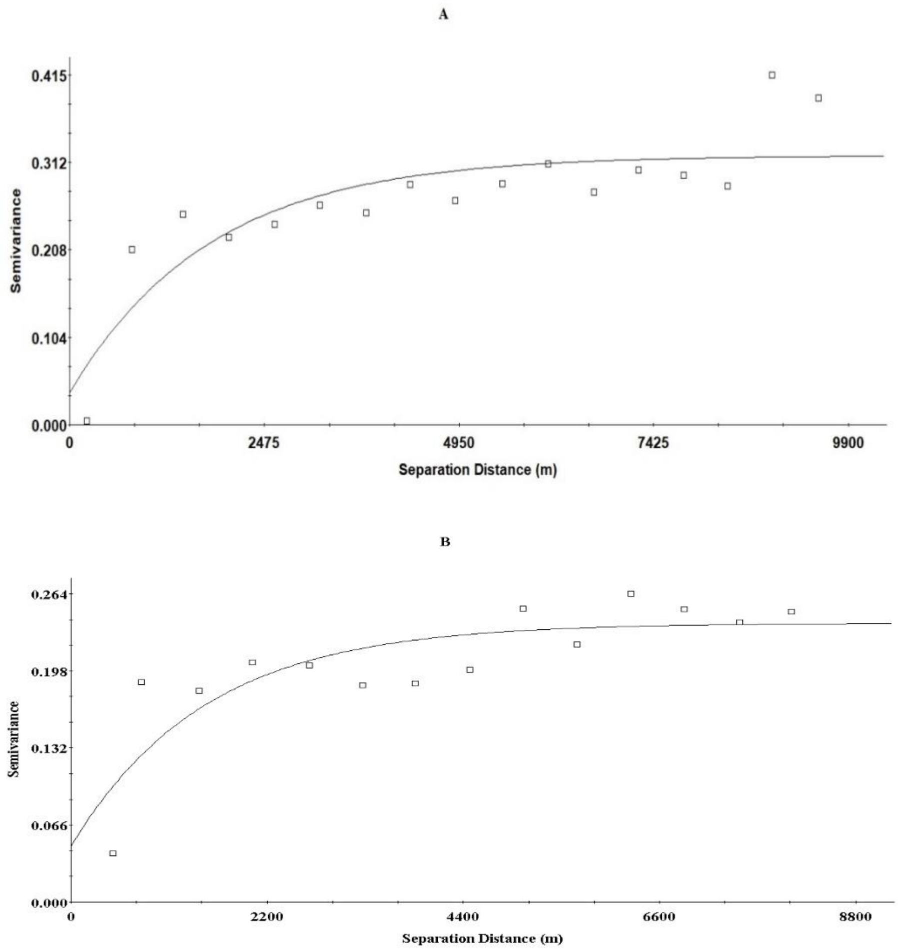


**Fig. 5.** Best-fit isotropic semivariogram models (with search neighborhood=5) of tree density (A) and basal area (B).

The results showed that the means of tree density and basal area estimated by applying the geostatistical kriging method were very similar to those calculated from the ground-based inventory (Table 3). The estimation error for tree density using the kriging method is 12.8%, which is 8.6% lower than the estimation error obtained from ground-based sample plots (14%; Table 3). Accordingly, the basal area estimation error was reduced from 11% using georeferenced sample plots to 9.4% with the kriging technique, which is about a 14.5% reduction compared to the ground-based inventory (Table 3). The similarity between statistics derived from ground inventory data and those estimated via ordinary kriging confirms the reliability of geostatistical estimations (Akhavan & Kiadaliri 2010). The paired t-test comparing measured and estimated tree density and basal area in the training sample plots showed no significant differences for tree density ($t = 0.230$, $p$-value = 0.819, df = 81) or basal area ($t = 0.361$, $p$-value = 0.719, df = 81). These results demonstrate that ordinary kriging achieved reasonable accuracy in estimating density indices. The results of forest density estimation using Kriging method (Figs. 6 and 7) confirmed significant spatial variability in tree density and basal area across the study area. Tree density was highest in the western region, reaching 1,155 stem ha$^{-1}$, and lowest in the northern region, at 110 stem ha$^{-1}$ (Fig. 6). The highest area, which was 5,622.01 ha, was attributed to the tree density class of 110–319 stem ha$^{-1}$. On the other hand, the lowest area covered 10.82 ha with a density class of 737–946 stem ha$^{-1}$. Similarly, the basal area also showed marked spatial variation: from the highest of 35.81 m$^2$ ha$^{-1}$ in the eastern part to the lowest of 3.76 m$^2$ ha$^{-1}$ in the western portion of the study area (Fig. 7). Maximum land area-3,732.77 ha fell under basal area class 10.17–16.58 m$^2$ ha$^{-1}$, and minimum area-6.18 ha fell under the highest basal area class of 29.40–35.81 m$^2$ ha$^{-1}$. The effectiveness of ordinary kriging in estimating various forest attributes has been extensively demonstrated, highlighting its reliability and precision in forest resource management. As a widely used geostatistical tool, kriging excels in spatial interpolation, monitoring forest dynamics, and optimizing forest management decisions by capturing both natural and anthropogenic spatial patterns (Sukkuea & Heednacram 2022; Teresinha *et al.* 2023). Ordinary kriging is favored for its simplicity and lower error rates compared to more complex models like co-kriging, proving highly reliable in tasks such as mapping forest stand volume (Tiryana 2005; Silveira *et al.* 2019), estimating cork production areas (Montes *et al*. 2005), and determining basal area and tree height (Akhavan & Klein 2009). Its adaptability is evident in diverse ecological contexts, including forest canopy mapping (Vafaei *et al*. 2022) and coppice forest management, with strong spatial autocorrelation observed in stem density and crown cover (Rezaei *et al*. 2014). Comparative studies consistently confirm kriging's superiority over methods like IDW, particularly in estimating tree density in dense forests (Munyati & Sinthumule 2021) and mapping productivity in beech forests and coppice stands (Akhavan *et al*. 2010; Ahadi *et al*. 2017). Kriging has been very efficient in mapping diameter growth, tree mortality, and ingrowth in the studies of Kalbi *et al*. (2017); it is similarly reliable for estimating tree height variability within the complex dynamics of forest change, as carried out by Goergen *et al*. (2020). Its efficiency in spatial analysis, optimal grid design, and density prediction further underscores its crucial role in sustainable forest management (Raimundo *et al*. 2017; Luo *et al*. 2024). The importance of geostatistical methods, in particular, kriging, for effective forest management based on precise and unbiased estimates of forest attributes, is underlined in this study. These geostatistical methods will be of increasing relevance in researching the impacts of traditional management practices to support informed decisions in sustainable forest management and conservation. Future studies should focus on adapting these methods to different forest types and management systems to improve their precision and broader applicability.

**Table 2.** Validation results of kriging interpolation methods for predicting tree density and basal area.

| Interpolation method | Tree density | | | | Basal area | | | |
|---|---|---|---|---|---|---|---|---|
| | MAE (stem ha$^{-1}$) | rMAE (%) | RMSE (stem ha$^{-1}$) | rRMSE (%) | MAE (m$^2$ ha$^{-1}$) | rMAE (%) | RMSE (m$^2$ ha$^{-1}$) | rRMSE (%) |
| Ordinary kriging | 103 | 33.3 | 137 | 44.4 | 4.05 | 30.63 | 5.53 | 41.8 |
| Simple kriging | 120 | 38.8 | 164 | 53.0 | 4.64 | 35.15 | 5.89 | 44.6 |
| Global kriging | 104 | 33.8 | 139 | 44.9 | 4.11 | 31.08 | 5.58 | 42.2 |
| Disjunctive kriging | 120 | 38.8 | 164 | 53.0 | 4.59 | 34.76 | 5.85 | 44.3 |

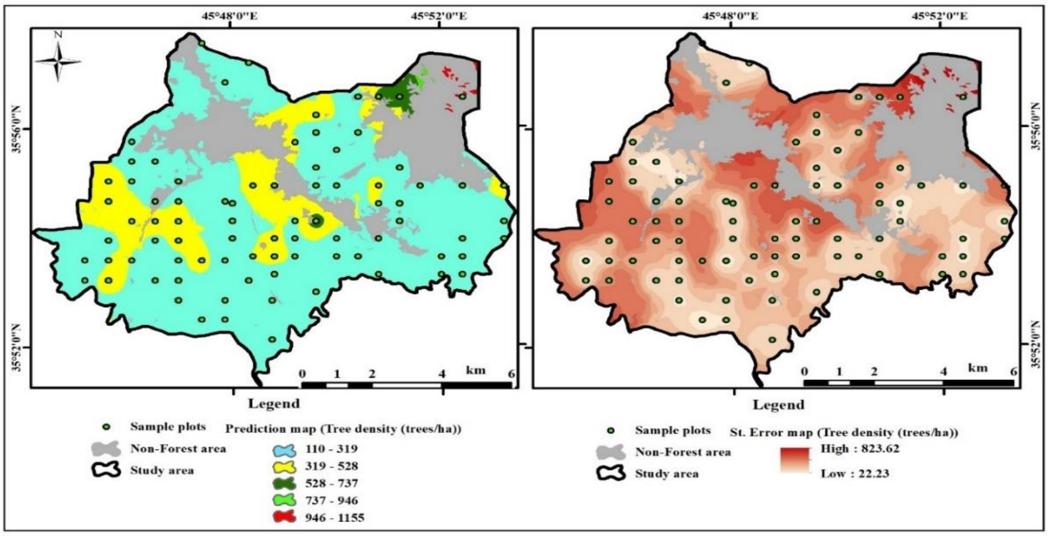


**Fig. 6.** Prediction map (A) and prediction standard error map (B) of tree density for the study area.

## CONCLUSION AND RECOMENDATIONS

This study highlighted the application and capability of geostatistical methods, particularly kriging interpolation, to assess the spatial distribution of tree density and basal area in pollarded oak forests in the Northern Zagros region of Iran. The findings revealed significant spatial variability in both tree density, averaging 291 stem ha$^{-1}$ with a coefficient of variation of 65.6%, and basal area, averaging 13.81 m² ha$^{-1}$ with a coefficient of variation of 49.9%. The observed dominance of small-diameter trees and clumped distribution patterns reflect historical management practices and localized environmental factors. Geostatistical analysis, including variogram modeling, confirmed strong spatial autocorrelation for both tree density and basal area, with high degrees of spatial dependence (88% for tree density and 82.2% for basal area). The exponential model and omnidirectional variograms for both variables proved effective for capturing spatial patterns, supporting the use of kriging techniques for accurate estimation. Ordinary kriging emerged as the most reliable interpolation method, with reasonable relative errors (rMAE = 33.3% for tree density, 30.63% for basal area) and no significant differences between measured and estimated values, though high rRMSE values indicated substantial variability and heterogeneity in the dataset.

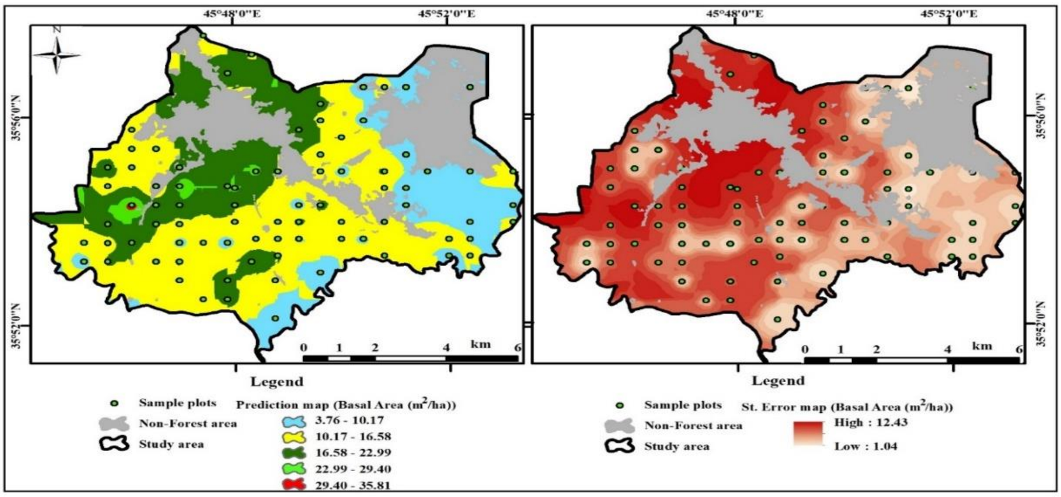


**Fig. 7.** Prediction map (A) and prediction standard error map (B) of basal area for the study area.

**Table 3.** Summary statistics of density indices at field sample plots and estimated using the ordinary kriging interpolation method.

| Estimation method | Attribute | n | Mean | SD | Min. | Max. | CV (%) | CS | CK | E (%) |
|---|---|---|---|---|---|---|---|---|---|---|
| Georeferenced sampling | Tree density (stem $ha^{-1}$) | 82 | 291 | 191 | 100 | 1200 | 65.6 | 2.4 | 7.5 | 14 |
| | Basal area ($m^2$ $ha^{-1}$) | 82 | 14.12 | 7.06 | 3.05 | 42.30 | 49.9 | 1.04 | 1.84 | 11 |
| Ordinary Kriging | Tree density (stem $ha^{-1}$) | 82 | 285 | 167 | 110 | 1155 | 58.6 | 2.5 | 9.4 | 12.9 |
| | Basal area ($m^2$ $ha^{-1}$) | 82 | 13.81 | 5.92 | 3.76 | 35.81 | 42.91 | 0.84 | 1.04 | 9.4 |

n: Sample Size; SD: Standard deviation; CV: Coefficient of variation; CS: Coefficient of asymmetry; CK: Coefficient of kurtosis; E: Error of estimate.

The similarity in the ground inventory data and ordinary kriging estimates, along with the non-significant differences in tree density and basal area from the paired t-test, serves to confirm that ordinary kriging is an accurate approach in the estimation of density indices. This study highlights how geostatistical approaches, particularly kriging, can transform forest resource management through spatially explicit decision-support systems. By accurately estimating critical stand parameters like tree density and basal area, this methodology provides forest managers with a powerful framework for sustainable ecosystem management that could be applied across comparable forest landscapes.

Based on the findings of this study, the following recommendations are provided to improve geostatistical techniques in pollarded oak forests:

1. Given the high variability and heterogeneity observed in tree density and basal area, increasing the sample size and utilizing stratified sampling methods are recommended. The latter can better represent different areas of the forest while considering environmental conditions and tree growth patterns. This approach can enhance the accuracy of geostatistical models and make spatial predictions more precise and reliable.

2. Considering the limitations of ordinary kriging, as indicated by the elevated rRMSE values suggesting potential for improved prediction accuracy, future research should focus on refining variogram modeling and exploring alternative kriging techniques to better capture complex spatial relationships. This would enhance the precision and comprehensiveness of forest assessments. To improve the accuracy of density and basal area estimations, survey intervals should be adjusted according to specific forest conditions, and advanced geostatistical methods, such as Co-Kriging, should be employed. By incorporating auxiliary variables, including spectral indices (i.e.

NDVI, EVI), soil fertility, and topography, Co-Kriging can improve predictive accuracy and reduce spatial heterogeneity.

**REFERENCES**


Abbasi, L, Shakeri, Z, Shabanian, N & Moreno, G 2017, Branch and leaf biomass of Lebanon oak (*Quercus libani* Oliv.) and gall oak (*Q. infectoria* Oliv.) trees in different years after pollarding. *Iranian Journal of Forest and Poplar Research*, 25: 46-35, [In Persian].

Achard, F, Mollicone, D, Stibig, HJ, Aksenov, D, Laestadius, L, Li, Z, Popatov, P & Yaroshenko, A 2006, Areas of rapid forest-cover change in boreal eurasia. *Forest Ecology and Management*, 237: 322-334.

Ahadi, Z, Alavi, J & Hoseini, M, 2017, Beech forest site productivity mapping using ordinary kriging and IDW (Case study: Research forest of Tarbiat Modares University). *Forest and Wood Products*, 70: 93-102, [In Persian].

Ahmed, C, Mohammed, A & Tahir, A 2020, Geostatistics of strength, modeling and GIS mapping of soil properties for residential purpose for Sulaimani City soils, Kurdistan Region, Iraq. *Modeling Earth Systems and Environment*, 6: 879-893.

Akhavan, R & Kleinn, C 2009, On the potential of kriging for estimation and mapping of forest plantation stock (case study: Beneshki plantation). *Iranian Journal of Forest and Poplar Research*, 17: 318-303, [In Persian].

Akhavan, R, ZahediAmiri, G & Zobeiri, M 2010, Spatial variability of forest growing stock using geostatistics in the Caspian region of Iran. *Caspian Journal of Environmental Sciences*, 8: 43-53.

Akhavan, R & Kia-Daliri, H 2010, Spatial variability and estimation of tree attributes in a plantation forest in the Caspian region of Iran using geostatistical analysis. *Caspian Journal of Environmental Sciences*, 8: 163-172.

Akhavan, R, Kia-Daliri, H & Etemad, V 2015, Geostatistically estimation and mapping of forest stock in a natural unmanaged forest in the Caspian region of Iran. *Caspian Journal of Environmental Sciences*, 13: 61-76.

Akhavan, R, Khanhasani, M & Khodakarami, Y 2018, Spatial patterns and inter-specific competition of three oak species in the Baneh forests of western Iran. *Forest and Wood Products*, 71: 149-159, [In Persian].

Alemu, B, Animut, G & Tolera, A 2013, Millettia ferruginea: an endemic legume tree as forage for ruminants in southern and northwestern Ethiopia. *Livestock Research for Rural Development*, 25.

Allard, D, Senoussi, R & Porcu, E 2016, Anisotropy models for spatial data. *Mathematical Geosciences*, 48: 305-328.

Appel, E, Barbosa, IC, Seidel, EJ & Oliveira, MSD 2018, Spatial dependence index for cubic, pentaspherical and wave semivariogram models. *Boletim de Ciências Geodésicas*, 24: 142-151.

Arétouyap, Z, Nouck, NP, Nouayou, R, Méli'i, JL, KemgangGhomsi, FE, PiepiToko, AD & Asfahani, J 2015, Influence of the variogram model on an interpolative survey using kriging technique. *Journal of Earth Science & Climatic Change*, 6: 316-316.

Azawi, H & Saleh, MS 2021, Review of the kriging technique applications to groundwater quality. *Journal of Engineering*, 27: 23-32.

Babcock, C, Finley, AO, Andersen, HE, Pattison, R, Cook, BD, Morton, DC, Alonzo, M, Nelson, R, Gregoire, T, Ene, L & Gobakken, T 2018, Geostatistical estimation of forest biomass in interior Alaska combining Landsat-derived tree cover, sampled airborne lidar and field observations. *Remote Sensing of Environment*, 212: 212-230.

Bargaoui, ZK & Chebbi, A 2009, Comparison of two kriging interpolation methods applied to spatiotemporal rainfall. *Journal of Hydrology*, 365: 56-73.

Berhe, DH & Tanga, AA 2013, Nutritional evaluation of Ficus thonningii Blume leaves as ruminant livestock feed in the Ahferom district of Tigray, Ethiopia. *African Journal of Range & Forage Science*, 30: 149-154.

Bhunia, GS, Keshavarzi, A, Shit, PK, Omran, ESE & Bagherzadeh, A 2018, Evaluation of groundwater quality and its suitability for drinking and irrigation using GIS and geostatistics techniques in semiarid region of Neyshabur, Iran. *Applied Water Science*, 8: 1-16.

Bivand, R 2008, Applied spatial data analysis with R. *Springer*, New York, USA, 374 p.

Bivand, RS 2009, Exploratory spatial data analysis. In: Handbook of Applied Spatial Analysis: Software Tools, Methods and Applications. Springer, Berlin, Germany, pp. 219-254.

Bonan, GB 2008, Forests and climate change: forcings, feedbacks, and the climate benefits of forests. *Science*, 320: 1444-1449.

Borel, R & Romero, F 1991, On-farm research in a silvopastoral project: a case study. *Agroforestry Systems*, 15: 245-257.

Buongiorno, J, Halvorsen, EA, Bollandsås, OM, Gobakken, T & Hofstad, O 2012, Optimizing management regimes for carbon storage and other benefits in uneven-aged stands dominated by Norway spruce, with a derivation of the economic supply of carbon storage. *Scandinavian Journal of Forest Research*, 27: 460-473.

Burner, DM, Pote, DH & Ares, A 2005, Management effects on biomass and foliar nutritive value of *Robinia pseudoacacia* and *Gleditsia triacanthos* f. inermis in Arkansas, USA. *Agroforestry Systems*, 65: 207-214.

Cambardella, CA, Moorman, TB, Novak, JM, Parkin, TB, Karlen, DL, Turco, RF.& Konopka, AE 1994, Field-scale variability of soil properties in central Iowa soils. *Soil Science Society of America Journal*, 58: 1501-1511.

Chiles, JP & Delfiner, P 2012, Geostatistics: modeling spatial uncertainty. *John Wiley & Sons*, Hoboken, USA, 713 p.

Dalchiavon, FC, dePassoseCarvalho, M, Andreotti, M & Montanari, R 2012, Spatial variability of the fertility attributes of Dystropheric Red Latosol under a no-tillage system. *Revista Ciência Agronômica*, 43: 453.

Diodato, N 2005, Geostatistical uncertainty modelling for the environmental hazard assessment during single erosive rainstorm events. *Environmental Monitoring and Assessment*, 105: 25-42.

Fattahi, M 1994, Study of western Iranian oak forests and their main degradation causes. *Research Institute of Forest and Rangeland*, Tehran, Iran, 210 p., [In Persian].

Freeman, EA & Moisen, GG 2007, Evaluating kriging as a tool to improve moderate resolution maps of forest biomass. *Environmental Monitoring and Assessment*, 128: 395-410.

Franzel, S, Carsan, S, Lukuyu, B, Sinja, J & Wambugu, C 2014, Fodder trees for improving livestock productivity and smallholder livelihoods in Africa. *Current Opinion in Environmental Sustainability*, 6: 98-103.

Ganawa, ESM, Soom, MAM, Musa, MH, Shariff, AM & Wayayok, A 2003, Spatial variability of total nitrogen and available phosphorus of large rice field in Sawah Sempadan Malaysia. *Science Asia*, 29: 7-12.

Gazolla-Neto, A, Fernandes, MC, Vergara, RDO, Gadotti, GI & Villela, FA 2016, Spatial distribution of the chemical properties of the soil and of soybean yield in the field. *Revista Ciência Agronômica*, 47: 325-333.

Geta, T, Nigatu, L & Animut, G 2014, Evaluation of potential yield and chemical composition of selected indigenous multi-purpose fodder trees in three districts of Wolayta Zone, Southern Ethiopia. *World Applied Sciences Journal*, 31: 399-405.

Ghahramany, L, Shakeri, Z, Ghalavand, E & Ghazanfari, H 2017, Does diameter increment of Lebanon oak trees (*Quercus libani* Oliv.) affected by pollarding in Northern Zagros, Iran? *Agroforestry Systems*, 91: 741-748.

Ghahramany, L, Ghazanfari, H, Fatehi, P & Valipour, A 2018, Structure of pollarded oak forest in relation to aspect in Northern Zagros, Iran. *Agroforestry Systems*, 92: 1567-1577, [In Persian].

Ghazanfari, H, Namiranian, M, Sobhani, H & Mohajer, RM 2004, Traditional forest management and its application to encourage public participation for sustainable forest management in the northern Zagros Mountains of Kurdistan Province, Iran. *Scandinavian Journal of Forest Research*, 19: 65-71.

Goergen, LCDG, Narvaes, IDS, Miquelutti, DJ, Chang, SX & Silva, EA 2020, Geostatistical behavior of dendrometric variables of Eucalyptus benthamii for forest management purpose. *Scientia Forestalis*, 48: 1-15.

GoldenSoftware 2025, Anisotropy, Golden Software Documentation. Available online: https://surferhelp.goldensoftware.com/griddata/Anisotropy.htm (accessed January 2, 2025).

Günlü, A, Bulut, S, Keleş, S & Ercanlı, İ 2020, Evaluating different spatial interpolation methods and modeling techniques for estimating spatial forest site index in pure beech forests: a case study from Turkey. *Environmental Monitoring and Assessment*, 192: 1-11.

Gunnarsson, F, Holm, S, Holmgren, P & Thuresson, T 1998, On the potential of kriging for forest management planning. *Scandinavian Journal of Forest Research*, 13: 237-245.

Harris, TM 2017, Exploratory spatial data analysis: tight coupling data and space, spatial data mining, and hypothesis generation. In: Regional Research Frontiers, Vol. 2: Methodological Advances, Regional Systems Modeling and Open Sciences. Springer, Cham, Switzerland, pp. 181-191.

Hawchar, L, ElSoueidy, CP & Schoefs, F 2018, Global kriging surrogate modeling for general time-variant reliability-based design optimization problems. *Structural and Multidisciplinary Optimization*, 58: 955-968.

Hemingway, H & Opalach, D 2024, Integrating lidar canopy height models with satellite-assisted inventory methods: a comparison of inventory estimates. *Forest Science*, 70: 2-13.

Hengl, T, Heuvelink, GB & Rossiter, DG 2007, About regression-kriging: from equations to case studies. *Computers & Geosciences*, 33: 1301-1315.

Heuvelink, GB 1998, Error propagation in environmental modelling with GIS. *CRC Press*, Boca Raton, USA, 150 p.

Humagain, K, Portillo-Quintero, C, Cox, RD & CainIII, JW 2017, Mapping tree density in forests of the southwestern USA using Landsat 8 data. *Forests*, 8: 287.

Hernandez, J & Emery, X 2009, A geostatistical approach to optimize sampling designs for local forest inventories. *Canadian Journal of Forest Research*, 39: 1465-1474.

Huang, YF, Ding, Y, Zang, RG, Li, XC, Zou, ZC & Han, WT 2012, Spatial pattern of trees in tropical lowland rain forest in Bawangling of Hainan Island, China. *Chinese Journal of Plant Ecology*, 36: 269-280.

Husch, B, Beers, TW & Kershaw JA 2002, Forest mensuration. *John Wiley & Sons*, Hoboken, USA, 456 p.

Hurteau, MD., 2021, The role of forests in the carbon cycle and in climate change. In: *Climate Change*. Elsevier, Amsterdam, Netherlands, pp. 561-579.

Izadi, S & Sohrabi, H 2022, Estimating the spatial distribution of above-ground carbon of Zagros forests using regression kriging, geographically weighted regression kriging and Landsat 8 imagery. *Journal of Geomatics Science and Technology*, 9: 113-124. [In Persian].

Jazirei, MH. & Ebrahimi Rostaghi, M 2003, Silviculture in Zagros forest. *Tehran University Press*, Tehran, Iran, 400 p. [In Persian].

John, K, Afu, SM, Isong, IA, Aki, EE, Kebonye, NM, Ayito, EO, Chapman, PA, Eyong, MO & Penížek, V 2021, Mapping soil properties with soil-environmental covariates using geostatistics and multivariate statistics. *International Journal of Environmental Science and Technology*, 18: 1-16.

Kalbi, S, Fallah, A, Shataee, S, Yousefpour, R & Bettinger, P 2017, Mapping the spatial distribution of forest growth characteristics using different geostatistical methods (case study: District No. 3, Sangdeh-Sari). *Iranian Journal of Forest and Poplar Research*, 25: 196-208, [In Persian].

Karami, O, Fallah, A, Shataei, SH & Latifi, H 2018, Assessment of geostatistical and interpolation methods for mapping forest dieback intensity in Zagros forests. *Caspian Journal of Environmental Sciences*, 16: 71-84.

Khedri, L, Ghahramany, L, Ghazanfari, H & Pulido, F 2017, A quantitative study of pollarding process in silvopastoral systems of Northern Zagros, Iran. *Forest Systems*, 26: e018.

Khosravi, S, Namiranian, M, Ghazanfari, H & Shirvani, A 2012, Estimation of leaf area index and assessment of its allometric equations in oak forests: Northern Zagros, Iran. *Journal of Forest Science*, 58: 116-122.

Klobučar, D. & Pernar, R 2012, Geostatistical approach to spatial analysis of forest damage. *Periodicum Biologorum*, 114: 103-110.

Li, J. & Heap, AD 2014, Spatial interpolation methods applied in the environmental sciences: a review. *Environmental Modelling & Software*, 53: 173-189.

Luo, P, Song, Y, Li, W & Meng, L 2024, Pervasive impact of spatial dependence on predictability. *arXiv Preprint arXiv:2408.14722*.

Ma, C 2007, Why is isotropy so prevalent in spatial statistics? *Proceedings of the American Mathematical Society*, 135: 865-871.

Marvi Mohajer, MR 2005, Silviculture. Tehran University Press, Tehran, Iran, 500 p., [In Persian].

Maselli, F & Chiesi, M 2006, Evaluation of statistical methods to estimate forest volume in a Mediterranean region. *IEEE Transactions on Geoscience and Remote Sensing*, 44: 2239-2250.

Myers, JC 1997, Geostatistical error management: quantifying uncertainty for environmental sampling and mapping. *John Wiley & Sons*, New York, USA, 350 p.

Meyer, S, Blaschek, M, Duttmann, R & Ludwig, R 2016, Improved hydrological model parametrization for climate change impact assessment under data scarcity—the potential of field monitoring techniques and geostatistics. *Science of the Total Environment*, 543: 906-923.

Miao, C & Wang, Y 2024, Interpolation of non-stationary geo-data using kriging with sparse representation of covariance function. *Computers and Geotechnics*, 169: 106183.

Mitas, L & Mitasova, H 1999, Spatial interpolation. In: *Geographical Information Systems: Principles, Techniques, Management and Applications*, Vol. 1. Wiley, New York, USA, pp. 481-492.

Montes, F, Hernández, MJ & Cañellas, I 2005, A geostatistical approach to cork production sampling estimation in *Quercus suber* forests. *Canadian Journal of Forest Research*, 35: 2787-2796.

Mulder, VL, De Bruin, S, Weyermann, J, Kokaly, RF & Schaepman, ME 2013, Characterizing regional soil mineral composition using spectroscopy and geostatistics. *Remote Sensing of Environment*, 139: 415-429.

Munyati, C. & Sinthumule, NI 2021, Comparative suitability of ordinary kriging and inverse distance weighted interpolation for indicating intactness gradients on threatened savannah woodland and forest stands. *Environmental and Sustainability Indicators*, 12: 100151.

Negreiros, J, Painho, M, Aguilar, F & Aguilar, M 2010, Geographical information systems principles of ordinary kriging interpolator. *Journal of Applied Sciences*, 10: 852-867.

Nanos, N, Calama, R, Montero, G & Gil, L 2004, Geostatistical prediction of height/diameter models. *Forest Ecology and Management*, 195: 221-235.

Newton, PF 2012, A decision-support system for forest density management within upland black spruce stand-types. *Environmental Modelling & Software*, 35: 171-187.

Oliver, MA & Webster, R 1990, Kriging: a method of interpolation for geographical information systems. *International Journal of Geographical Information System*, 4: 313-332.

Oliver, MA, Webster, R & McGrath, SP 1996, Disjunctive kriging for environmental management. *Environmetrics*, 7: 333-357.

Olthoff, AE, Gómez, C, Alday, JG & Martínez-Ruiz, C 2018, Mapping forest vegetation patterns in an Atlantic–Mediterranean transitional area by integration of ordination and geostatistical techniques. *Journal of Plant Ecology*, 11: 114-122.

Pascual, C, Mauro, F, Hernando, A & Martín-Fernández, S 2013, Inventory techniques in participatory forest management. Quantitative techniques in participatory forest management. CRC Press, Boca Ratón, pp. 53-134.

Peri, PL, Bahamonde, HA, Lencinas, MV, Gargaglione, V, Soler, R, Ormaechea, S & Pastur, GM 2016, A review of silvopastoral systems in native forests of Nothofagus antarctica in southern Patagonia, Argentina. *Agroforestry Systems*, 90: 933-960.

Pelissari, AL, Roveda, M, Caldeira, SF, Sanquetta, CR, Corte, APD & Rodrigues, CK 2017, Geostatistical modeling of timber volume spatial variability for Tectona grandis LF precision forestry. *Cerne*, 23: 115-122.

Pinkard, EA, Battaglia, M, Beadle, CL & Sands, PJ 1999, Modeling the effect of physiological responses to green pruning on net biomass production of Eucalyptus nitens. *Tree Physiology*, 19: 1-12.

Raimundo, MR, Scolforo, HF, de Mello, JM, Scolforo, JRS, McTague, JP & dos Reis, AA 2017, Geostatistics applied to growth estimates in continuous forest inventories. *Forest Science*, 63: 29-38.

Raju, NJ 2016, Geostatistical and geospatial approaches for the characterization of natural resources in the environment. Cham: Springer, 969 p.

Ranjbar, A, Ghahramani, L & Pourhashemi, M 2012, Impact assessment of pollarding on biometrical indices of Lebanon oak (Quercus libani Oliv.) in Belake Forests, Baneh. *Iranian Journal of Forest and Poplar Research*, 20: 578-594 (In Persian).

Ray, D, Seymour, R, Fraver, S, Berrill, JP, Kenefic, L, Rogers, N & Weiskittel, A 2023, Relative density as a standardizing metric for the development of size-density management charts. *Journal of Forestry*, 121: 443-456.

Rawat, YS & Everson, CS 2013, Availability and use of willow species in representative cold desert areas of northwestern himalaya, India. *Journal of Mountain Science*, 10: 472-481.

Rehman, S, Sajjad, H, Masroor, M, Rahaman, MH, Roshani, Ahmed, R & Sahana, M 2022, Assessment of evidence-based climate variability in Bhagirathi sub-basin of India: a geostatistical analysis. *Acta Geophysica*, 70: 445-463.

Reza, SK, Nayak, DC, Mukhopadhyay, S, Chattopadhyay, T & Singh, SK 2017, Characterizing spatial variability of soil properties in alluvial soils of India using geostatistics and geographical information system. *Archives of Agronomy and Soil Science*, 63: 1489-1498.

Rezaei, E, Akhavan, R, Soosani, J & Pourhashemi, M 2014, Efficiency of kriging for estimation and mapping of crown cover and density of Zagros Oak forests (Case study: Dadabad Region, Khorramabad). *Forest and Wood Products*, 67: 359-370, [In Persian].

Rojimol, J, Phanindra, KBVN & Umashankar, B 2021, Application of ordinary kriging for in situ site characterization. In Proceedings of the Indian Geotechnical Conference 2019: IGC-2019 Volume V, Springer Singapore, pp. 551-563.

Rostami Jalilian, A, Ghahramany, L, Ghazanfari, H & Shakeri, Z 2016, Response of Gall oak (*Quercus infectoria* Oliv.) to pollarding in northern Zagros. *Iranian Journal of Forest and Poplar Research*, 24: 633-645, [In Persian].Rozas, V, Zas, R & Solla, A 2009, Spatial structure of deciduous forest stands with contrasting human influence in northwest Spain. *European Journal of Forest Research*, 128: 273-285.

Safari, A, Shabanian, N, Heidari, RH, Erfanifard, SY & Pourreza, M 2010, Spatial pattern of Manna oak trees (*Quercus brantii* Lindl.) in Bayangan forests of Kermanshah. *Iranian Journal of Forest and Poplar Research*, 18(4):608-596, [In Persian].

Sales, MH, SouzaJr, CM, Kyriakidis, PC, Roberts, DA & Vidal, E 2007, Improving spatial distribution estimation of forest biomass with geostatistics: A case study for Rondônia, Brazil. *Ecological Modelling*, 205(1-2): 221-230.

Schiappapietra, E & Douglas, J 2020, Modelling the spatial correlation of earthquake ground motion: Insights from the literature, data from the 2016–2017 Central Italy earthquake sequence and ground-motion simulations. *Earth-Science Reviews*, 203:103139.

Scott, CT & Gove, JH 2002, Forest inventory. *Encyclopedia of Environmetrics*, 2:814-820.

Selmy, S., AbdEl-Aziz, S., El-Desoky, A. & El-Sayed, M 2022, Characterizing, predicting, and mapping of soil spatial variability in Gharb El-Mawhoub area of Dakhla Oasis using geostatistics and GIS approaches. *Journal of the Saudi Society of Agricultural Sciences*, 21(6): 383-396.

Shahabedini, S, Ghahramany, L, Pulido, F, Khosravi, S & Moreno, G 2018, Estimating leaf biomass of pollarded Lebanon oak in open silvopastoral systems using allometric equations. *Trees*, 32: 99-108.

She, GH, Lin, GZ, Wen, XR, Lin, SM & Ye, J S2007, Improvement of forest inventory method for management plan and stand growth estimation on horizontal point sample. *Journal of Nanjing Forestry University*, 50(05): 11.

Silveira, EM, Reis, AA, Terra, MC, Withey, KD, Mello, JM, Acerbi-Junior, FW & FerrazFilho, AC 2019, Spatial distribution of wood volume in Brazilian savannas. *Anais da Academia Brasileira de Ciências*, 91: e20180666.

Siviero, E, Chautru, E & Clémençon, S 2024, A statistical learning view of simple Kriging. *TEST*, 33(1):271-296.

Sukkuea, A & Heednacram, A 2022, Prediction on spatial elevation using improved kriging algorithms: An application in environmental management. *Expert Systems with Applications*, 207: 117971.

Svidzinska, D 2019, The application of directional univariate structure functions analysis for studying the spatial anisotropy of environmental variables. *Ekológia (Bratislava)*, 38(2): 140-153.

Thonon, I. & CacheiroPose, M 2001, Geostatistical interpolation of topographical field data in order to obtain a DEM of a small forest catchment in Northwest Spain. *Cadernos do Laboratorio Xeolóxico de Laxe*, 26: 179-190.

Tiryana, T 2005, Predicting spatial distribution of stand volume using geostatistics. *Jurnal Manajemen Hutan Tropika*, 11(2): 15-27.

Vafaei, S, Maleknia, R, Naghavi, H & Fathizadeh, O 2022, Estimation of forest canopy using remote sensing and geostatistics (case study: Marivan Baghan Forests). *J Environ Sci Technol*, 24: 71-82, [In Persian].

Valipour, A, Plieninger, T, Shakeri, Z, Ghazanfari, H, Namiranian, M & Lexer, MJ 2014, Traditional silvopastoral management and its effects on forest stand structure in northern Zagros, Iran. *Forest Ecology and Management*, 327: 221-230.

Villegas, P, Cavagna, A, Cencini, M, Fort, H & Grigera, TS2021, Joint assessment of density correlations and fluctuations for analysing spatial tree patterns. *Royal Society Open Science*, 8(1):202200.

Verbovšek, T 2024, Analysis of Karst surface anisotropy using directional semivariograms, Slovenia. *Pure and Applied Geophysics*, 181(1): 233-245.

Wackernagel, H 1996, Multivariate geostatistics: An introduction with applications. In *International Journal of Rock Mechanics and Mining Sciences and Geomechanics Abstracts*, 8(33): 363A.

WalterIII, JF, Christman, MC, Hoenig, JM & Mann, R 2007, Combining data from multiple years or areas to improve variogram estimation. *Environmetrics: The Official Journal of the International Environmetrics Society*, 18(6): 583-598.

Webster, R & Oliver, MA 2007, Geostatistics for environmental scientists. John Wiley & Sons.

Woodall, CW, D'Amato, AW, Bradford, JB & Finley, AO 2012, Stand density index as a tool to assess the maximization of forest carbon and biomass. In: McWilliams, Will; Roesch, Francis A. eds., Monitoring Across Borders: 2010 Joint Meeting of the Forest Inventory and Analysis (FIA) Symposium and the Southern Mensurationists, e-Gen. Tech. Rep. SRS-157. Asheville, NC: US Department of Agriculture, Forest Service, Southern Research Station, pp. 293-296.

Wu, Z, Yao, F, Zhang, J & Liu, H 2024, Estimating forest aboveground biomass using a combination of geographical random forest and empirical Bayesian kriging models. *Remote Sensing*, 16(11): 1859.

Yadav, BK & Nandy, S 2015, Mapping aboveground woody biomass using forest inventory, remote sensing and geostatistical techniques. *Environmental Monitoring and Assessment*, 187: 1-12.

Zhao, Z, Feng, Z, Liu, J & Wang, Y 2022, Development and testing of a new UWB positioning measurement tool to assist in forest surveys. *Sustainability*, 14(24): 17042.